

Article

Contrasting Changes in Vegetation Growth due to Different Climate Forcings over the Last Three Decades in the Selenga-Baikal Basin

Guan Wang^{1,2}, Ping Wang^{1,*} , Tian-Ye Wang^{1,2} , Yi-Chi Zhang¹, Jing-Jie Yu^{1,2}, Ning Ma³, Natalia L. Frolova⁴ and Chang-Ming Liu¹

¹ Key Laboratory of Water Cycle and Related Land Surface Processes, Institute of Geographic Sciences and Natural Resources Research, Chinese Academy of Sciences, Beijing 100101, China;

wangg.16b@igsnr.ac.cn (G.W.); wangty.16b@igsnr.ac.cn (T.-Y.W.); zhangych@reis.ac.cn (Y.-C.Z.); yujj@igsnr.ac.cn (J.-J.Y.); liucm@igsnr.ac.cn (C.-M.L.)

² University of Chinese Academy of Sciences, Beijing 100049, China

³ Key Laboratory of Tibetan Environment Changes and Land Surface Processes, Institute of Tibetan Plateau Research, Chinese Academy of Sciences, Beijing 100101, China; ningma@itpcas.ac.cn

⁴ Department of Land Hydrology, Lomonosov Moscow State University, GSP-1, Leninskie Gory, Moscow 119991, Russia; frolova_nl@mail.ru

* Correspondence: wangping@igsnr.ac.cn; Tel.: +86-10-6488-9732

Received: 2 January 2019; Accepted: 16 February 2019; Published: 19 February 2019



Abstract: The Selenga-Baikal Basin, a transboundary river basin between Mongolia and Russia, warmed at nearly twice the global rate and experienced enhanced human activities in recent decades. To understand the vegetation response to climate change, the dynamic spatial-temporal characteristics of the vegetation and the relationships between the vegetation dynamics and climate variability in the Selenga-Baikal Basin were investigated using the Normalized Difference Vegetation Index (NDVI) and gridded temperature and precipitation data for the period of 1982 to 2015. Our results indicated that precipitation played a key role in vegetation growth across regions that presented multiyear mean annual precipitation lower than 350 mm, although its importance became less apparent over regions with precipitation exceeding 350 mm. Because of the overall temperature-limited conditions, temperature had a more substantial impact on vegetation growth than precipitation. Generally, an increasing trend was observed in the growth of forest vegetation, which is heavily dependent on temperature, whereas a decreasing trend was detected for grassland, for which the predominant growth-limiting factor is precipitation. Additionally, human activities, such as urbanization, mining, increased wildfires, illegal logging, and livestock overgrazing are important factors driving vegetation change.

Keywords: climate change; vegetation growth; NDVI; Baikal Lake; vegetation response

1. Introduction

Average global surface temperature has increased over the past century, and precipitation has decreased in most mid-latitude and arid areas [1,2]. Climate change has a considerable effect on the hydrological cycle by altering the amount and distribution characteristics of global water resources [3]. According to recent studies [4–10], changes in the global climate over the past century have also greatly impacted terrestrial ecosystems worldwide, and Eurasia has been especially strongly affected [11,12]. Significantly greater temperature increases than the global average and variable precipitation have been observed in this region, particularly in the Selenga-Baikal Basin [13].

As the key component of terrestrial ecosystems and an important medium for energy exchange and water and biogeochemical cycles, the vegetation dynamics of terrestrial ecosystems have been recognized as one of the most significant environmental issues related to climate change [14,15]. Changes in climate affect vegetation growth by altering the exchange of mass and energy between the atmosphere and vegetation, and the consequences are evident through geographical differences in vegetation growth. For example, a slight upward trend in vegetation greenness was detected in the eastern part of Central Asia from 1984 to 2013, while a slight downward trend was detected in the western part [2].

In general, vegetation growth primarily depends on three climatic factors; i.e., temperature, precipitation, and radiation, and they can explain 64% of the global variation in vegetation for the 1982–2008 period [16]. Temperature is the major limiting factor at high latitudes [17], precipitation is the dominant factor in arid and semiarid regions, and radiation plays a vital role in the dynamics of tropical rainforests [18–21]. The Selenga-Baikal Basin, a transboundary basin between Mongolia and Russia with a semiarid climate, has experienced almost twice the global average warming over the 20th century [22] and most of the regions throughout this basin have also shown decreasing annual precipitation in recent decades [23]. Climate change in this region is likely to have an appreciable effect on vegetation dynamics, such as the degradation of grassland steppe in the southern Selenga-Baikal Basin in Mongolia [24]. As a consequence, understanding the response of the vegetation in the Selenga-Baikal Basin to climate change has become highly important.

Recently, the effects of climate change on vegetation dynamics in the Selenga-Baikal Basin have attracted the attention of the public in addition to that of scientists and governments worldwide [22], particularly in association with the protection of the deepest and largest freshwater reservoir on Earth, Lake Baikal, which has been declared a UNESCO World Heritage Site due to its unique ecosystems [25]. However, our understanding of the vegetation dynamics and their responses to climate change within the entire Selenga-Baikal Basin, where the rate of warming is almost twice the global rate over past decades [22,26], is limited. Therefore, this study aims to further (1) characterize the temporal change trends and spatial patterns of climate variables and vegetation across the Selenga-Baikal Basin from 1982 to 2015; (2) identify the effects of the predominant climatic factors; i.e., temperature and precipitation, on vegetation growth under different conditions; and (3) distinguish the various responses of grassland and forest to climatic factors and human disturbances.

2. Materials and Methods

2.1. Study Area

The Selenga-Baikal Basin ($46^{\circ}28'–56^{\circ}42'E$, $96^{\circ}52'–113^{\circ}50'N$) is located in the central part of the Eurasian continent along the international boundary between Mongolia and Russia (Figure 1). The total area of the basin is $\sim 570,000$ km², with 44.6% situated within Russia and 55.4% within Mongolia [27]. Two lakes are located within the study area (Figure 1). Lake Khovsgol is the largest freshwater lake in Mongolia by volume and the second largest by surface area. Lake Baikal is the largest lake in the world and holds 20% of the world's total unfrozen freshwater reserve, and it can essentially be regarded as a freshwater sea [27,28]. The Selenga, Upper Angara, and Barguzin rivers are the major tributaries of Lake Baikal.

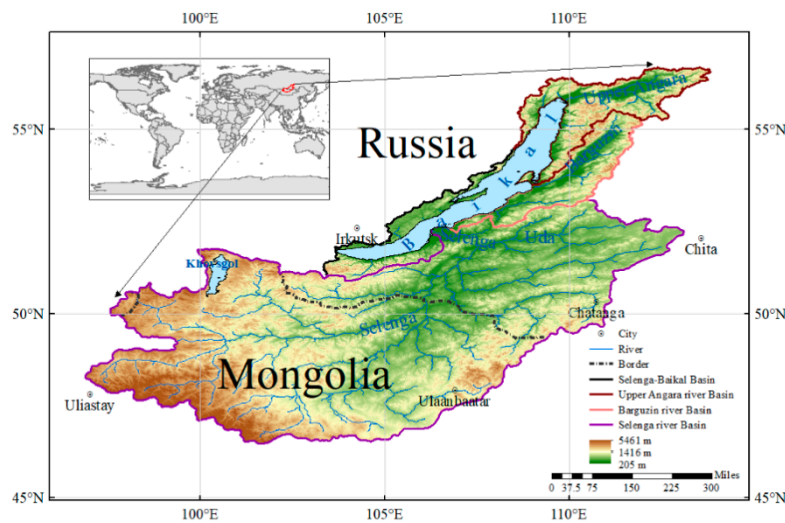


Figure 1. Topographical map of the Selenga-Baikal Basin.

The Selenga-Baikal Basin is characterized by an extremely continental climate with considerable annual and daily fluctuations in air temperature and an uneven seasonal precipitation distribution. The basin is distinguished by long, cold winters, during which the air temperatures at Lake Baikal reach $-37\text{ }^{\circ}\text{C}$ to $-40\text{ }^{\circ}\text{C}$, and the lake freezes for four to five months each year. Snow usually falls from mid-October to mid-April, and the mountains remain covered in snow and frozen until approximately early April [29,30]. In addition, the summer air temperatures soar briefly to $25\text{ }^{\circ}\text{C}$ to $30\text{ }^{\circ}\text{C}$ in this strongly continental climate [31]. Substantial spatial variation in precipitation is observed across the watershed, and more than half of the annual precipitation occurs during summer (June–August) [28]. The basin is subjected to harsh climate conditions and governed by its mountain permafrost terrain, with permafrost ranging from isolated patches in the middle part of the basin to continuous permafrost in the mountainous parts [22].

The southern part of the Selenga-Baikal Basin in Mongolia is mainly covered by grassland with a low soil moisture content, while the middle part of the basin is covered by dense taiga vegetation [32]. In general, green-up begins in the middle of May for the forest, while the average onset date for grassland is the middle of June, and both grassland and forest reach peak NDVI values in late July. The average date for the onset of dormancy for both forest and grassland in this area is in late September [33]. Recent studies have detected widespread degradation of the Mongolian steppe, and approximately 80% declines in NDVI could be explained by increasing livestock abundance [34].

2.2. Data Sources

2.2.1. Climate Data

Climate Research Unit (CRU) monthly temperature and precipitation data (version TS4.00) during the period from 1982 to 2015 at a spatial resolution of 0.5° (<http://www.cru.uea.ac.uk>) [35] were used in the study. Gridded datasets were generated by interpolating the records from more than 4000 meteorological stations worldwide using spatial autocorrelation functions [36,37]. CRU data have been widely applied in global climate studies [21,38,39], and the CRU climate data were resampled from 0.5° to 0.083° based on a bilinear interpolation to match the Global Inventory Monitoring and Modeling System (GIMMS) 3g NDVI data.

2.2.2. Land Cover Data

We used the Global Land Cover (GLC) 30-m dataset (GlobeLand30), which is derived from a Chinese GLC mapping project (www.globeland30.org) that provides GLC data at a spatial resolution of 30 m in 2000 and 2010 [40]. The GlobeLand30 classification utilized multispectral images from

the American Land Resources Satellite (Landsat) TM5/ETM+ and the China Environmental Disaster Alleviation Satellite (HJ-1) [41]. The total classification accuracy of GlobeLand30 was 83.5%, and the products have been widely used for studies of environmental change, land resource management, sustainable development, etc. [42,43]. In this study, we chose the remote sensing images from 2010 to classify the land cover types.

2.2.3. NDVI Data

We used the GIMMS 3g NDVI dataset acquired by the Advanced Very High Resolution Radiometer (AVHRR) and processed and archived by the National Aeronautics and Space Administration (NASA) (<https://ecocast.arc.nasa.gov/data/pub/gimms>). These data constitute the longest available NDVI dataset from 1982–2015 with spatial and temporal resolutions of 0.083° and 15 days, respectively. GIMMS 3g NDVI data have been widely utilized to monitor vegetation dynamics at the global and continental scales [44–49]. The 15-day data were transformed into monthly data to match the CRU climate data via the maximum value composite (MVC) method, which can largely remove atmospheric noise [50]. As noted by Beck, et al. [51], estimating the NDVI of high-latitude vegetation is problematic during winter due to the effects of snow. In this study, the NDVI was analyzed during the growing seasons from May to September according to Lavrentyeva, et al. [52]; therefore, the influence of snow was negligible.

2.3. Methods

2.3.1. Theil–Sen Median Trend Analysis

We performed a Theil–Sen median trend analysis combined with the Mann–Kendall test to identify trends in large sets of time series data; this combination has been used to analyze long time series of climate and vegetation data [2,53,54]. Because abnormal values have less influence, the Theil–Sen median trend analysis has been proven to be more suitable than linear regression [55–57], and the computational formula is as follows:

$$S = \text{Median} \left(\frac{x_j - x_i}{j - i} \right), i < j \quad (1)$$

where S is the Theil–Sen median slope; Median is the median of a set of data values; i and j represent the years; and x_i and x_j are the values of year i and j , respectively.

2.3.2. Mann–Kendall Test

The Mann–Kendall trend test [58,59] is a nonparametric statistical test used to assess the significance of the effects of climate on vegetation change [60], and it has been widely applied to analyze the trends and variations in hydrological and meteorological time series, as well as to investigate long meteorological and vegetation time series [61]. The advantage of this method is that the samples do not need to follow a certain distribution and are free from interference from a few outliers [58]. A significance level of 0.05 indicates a statistically significant variation if $|Z| > 1.96$. Combined with the Theil–Sen median trend analysis and the Mann–Kendall test, we divided the study area into improved ($S > 0$) and degraded regions ($S < 0$) and further determined whether the changes were significant ($Z \geq 1.96$ or $Z \leq -1.96$) or not ($-1.96 < Z < 1.96$).

2.3.3. Partial Correlation Analysis

The partial correlation coefficient is used to study the correlation between an independent variable and the dependent variable by excluding the impact of the other independent variables [62]. For this research, the dependent variable is the NDVI and the independent variables are temperature and

precipitation. We used the partial correlation coefficient to explore the correlation between the NDVI and single meteorological variables. The partial correlation coefficient is calculated as follows:

$$r_{x_1y \cdot x_2} = \frac{r_{x_1y} - r_{x_1x_2}r_{x_2y}}{\sqrt{(1 - r_{x_1x_2}^2)(1 - r_{x_2y}^2)}} \quad (2)$$

where $r_{x_1y \cdot x_2}$ is the partial correlation coefficient of variables x_1 and y excluding the effect of variable x_2 , and $r_{x_1x_2}$, r_{x_1y} , r_{x_2y} are the Pearson correlation coefficients between variables x_1 and x_2 , x_1 and y , and x_2 and y , respectively. The two-tailed t-test was used to estimate the significance of the calculated partial correlations, and $p < 0.05$ was considered significant.

3. Results

3.1. Meteorological Characteristics

3.1.1. Spatial Patterns of Air Temperature and Precipitation

As shown in Figure 2, air temperature and precipitation are highly spatially heterogeneous in the Selenga-Baikal Basin. The average annual air temperature over most of the region is below 0 °C and varies from −10.50 °C to 1.44 °C. The areas with relatively low air temperature are mainly located in the southwest and northeast of the basin, which represent the regions with high elevation and high latitude, respectively. Generally, the air temperature increases from high to low elevation, as well as from high to middle latitudes. Therefore, the spatial pattern of the annual air temperature distribution within the basin is essentially caused by the combined effects of elevation and latitude.

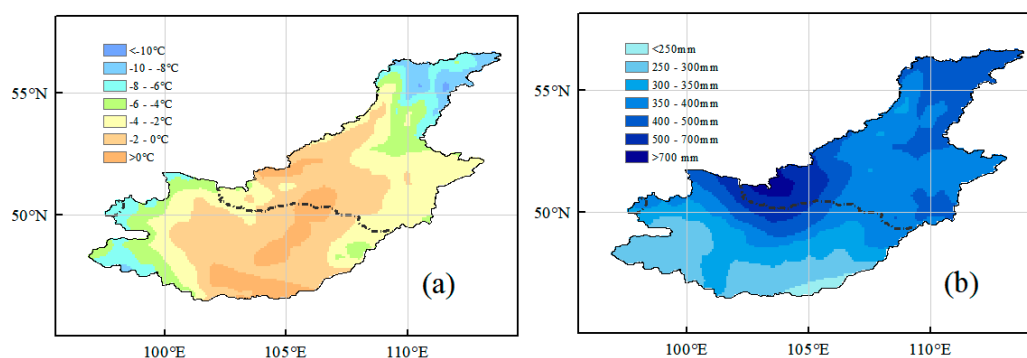


Figure 2. Spatial distribution of the average annual temperature (a) and precipitation (b) from 1982 to 2015.

Most of the basin is located in a semiarid area, and the annual precipitation is 383.9 mm. The annual average precipitation is very limited in the south of the basin and varies from 200 to 300 mm, whereas that in the intermountain depressions of the Uda and Selenga Rivers can reach 300–400 mm. Over the Upper Angara River Basin and the Barguzin Basin, the annual average precipitation is approximately 400–450 mm. The maximum amount of precipitation occurs over the northwestern wind-facing slopes of the ridges that bound Lake Baikal and primarily face toward the prevailing air currents. Overall, the highly uneven distribution of precipitation largely depends on the locations of mountains, which greatly influence the distribution of humidity and the amount of precipitation by controlling moisture-carrying air currents [63].

3.1.2. Temporal Variations in Air Temperature and Precipitation

Figures 3 and 4 show the spatial distribution of the annual and seasonal change trends of the average air temperature and total precipitation from 1982 to 2015, respectively. As shown in Figure 3a, the air temperature increased over the past three decades in all regions, and 51.82% of the regions

passed the significance test ($p < 0.05$). In general, the warming trend was increasingly obvious from the northeast to the southwest. The change trends in air temperature exhibited different patterns among seasons as shown in Figure 4, and a significant increasing trend can be observed in spring and summer. The winter temperature, in contrast, decreased during the 1982–2015 period, which is consistent with recent studies, e.g., [23,64,65]. However, the decreasing winter temperature trend in the Selenga-Baikal Basin did not pass a significance test at the 0.05 level.

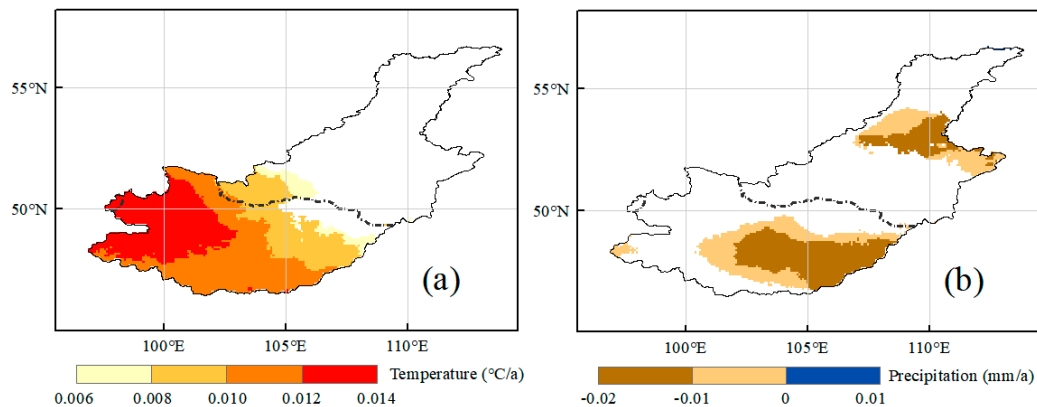


Figure 3. Spatial distribution of the change trends ($p < 0.05$) of the average annual temperature (a) and precipitation (b) over the Selenga-Baikal Basin from 1982 to 2015. The blank represents $p > 0.05$, which is not significant.

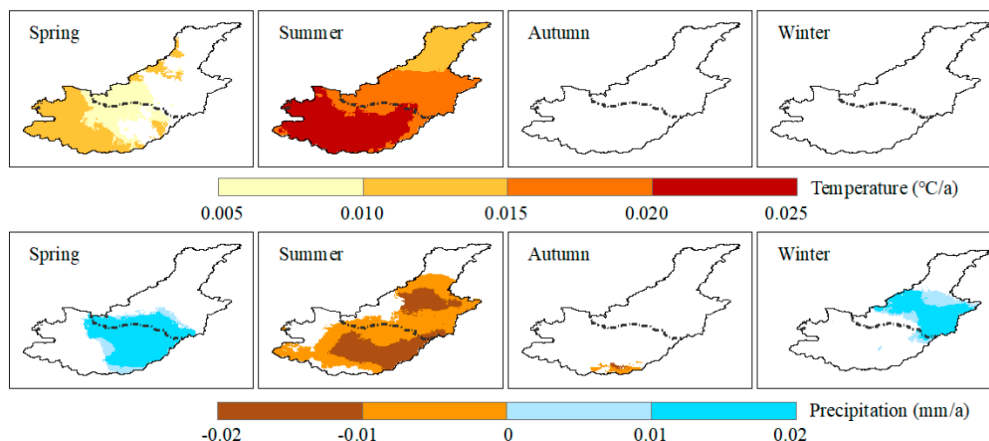


Figure 4. Spatial distribution of the change trends ($p < 0.05$) of the seasonal temperature (upper) and precipitation (lower) over the Selenga-Baikal Basin from 1982 to 2015.

The precipitation over most of the region showed a notable decreasing trend over the past three decades (Figure 3b). The precipitation presented spatial variability with decreasing trends in 95.40% of the regions, with 31.08% experiencing significant decreases. Regions in the eastern and southern parts of the study area presented notable declines in precipitation and the highest change rate of -0.013 mm/a, whereas the opposite trend was observed in the northeastern region, although this rate did not pass the significance test at the level of 0.05. In most regions, precipitation in the summer exhibited decreasing trends, while that in the winter and spring presented increasing trends (Figure 4). It is worth noting that the increase in total precipitation during spring and winter was not sufficient to offset the decrease in summer; therefore, the annual precipitation showed a decreasing trend with a spatial distribution similar to that of the annual precipitation in the summer.

3.2. Vegetation Condition and Change

3.2.1. Vegetation Condition

As shown in Figure 5, grassland, forest, water bodies, cultivated land, and bare land account for 51.05%, 36.91%, 6.48%, 3.54%, and 1.34% of the total basin, respectively, while other land use types account for less than 1%. Grassland, which occupies more than half of the entire basin, is the most predominant land cover and is mainly distributed throughout the Mongolian sector. Forest is another predominant land cover over 37% of the total area, and it is mainly distributed in the Russian parts. Cultivated land is mainly distributed in river-lined areas of the Uda River and the lower reaches of the Selenga River, and bare land is mainly distributed in the southern part of Mongolia. Below, we focus our analysis on forest and grassland.

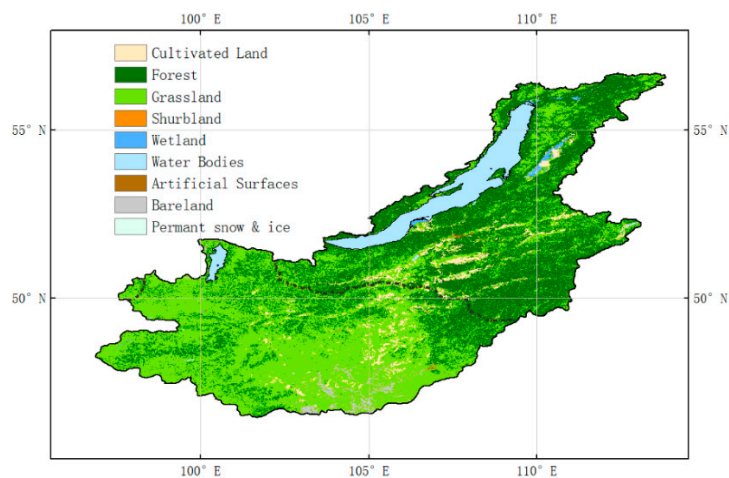


Figure 5. Spatial distribution of the different vegetation types in the Selenga-Baikal Basin based on GlobeLand30 in 2010.

The mean NDVI in the growing season (from May to September according to Lavrentyeva, Merkusheva and Ubugunov [52]) exhibited a spatially heterogeneous pattern from 1982 to 2015 (Figure 6a). As expected, the NDVI generally followed the spatial pattern of the vegetation types identified in this area with higher values in forested areas to the north and lower values in the grassland. The mean NDVI of forest, which was mainly distributed in the northwestern and southeastern parts of the Selenga-Baikal Basin, was 0.667. Grassland, which covered the southern part of the basin, had a relatively low mean NDVI (0.542).

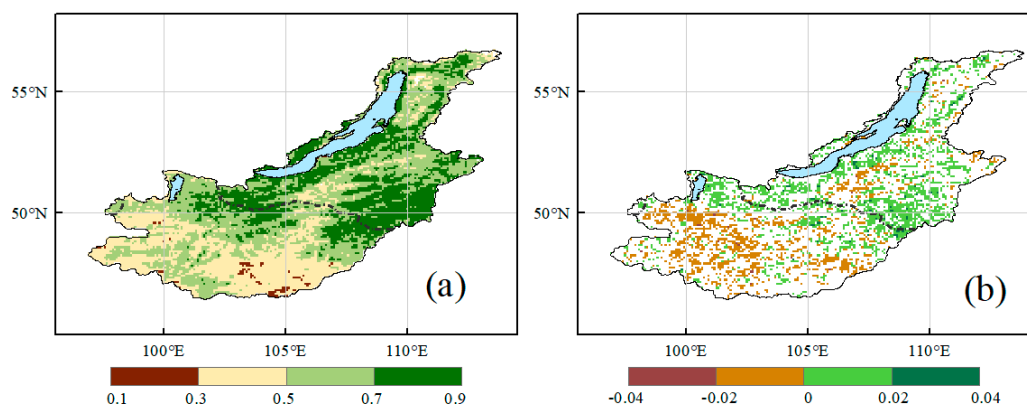


Figure 6. Spatial distribution of the (a) multiyear mean NDVI and (b) its trends ($p < 0.05$) during the growing season from 1982 to 2015.

3.2.2. Vegetation Change

As shown in Figure 6b, this basin showed various trends in NDVI from 1982 to 2015. A total of 21.74% of the region showed a significant increasing trend, while 14.35% of the area exhibited a significant decreasing trend, and the stable areas accounted for 63.91%. Moreover, the vegetation changes in the Selenga-Baikal Basin exhibited obvious regional characteristics. The changes in the mean NDVI during the growing season indicate vegetation greening along the abovementioned northwest-southeast strip in addition to the intermountain depressions and southeastern mountainous region. However, a decreasing trend in vegetation was mainly detected in the southern part of the Mongolian sector, suggesting that most of Mongolia has experienced remarkable vegetation degradation.

Changes in the annual vegetation growth of forest and grassland were equivalent based on a comparison of the monthly NDVI values for land cover types before and after 2000 (Figure 7). Forest and grassland degraded in the summer and improved in spring and autumn, but the degradation of grassland was more evident. In addition, the NDVI value in winter was affected by snow cover and thus could not accurately reflect vegetation growth; therefore, the change in winter is not discussed here. However, the NDVI change trends for the different types of vegetation varied recently over the past 30 years (Table 1). Forest showed significant increasing trends, with 30.19% of these areas showing a significant increasing trend and only 7.03% displaying a significant decreasing trend. It was worth noting that improved forest growth throughout the entire basin was mainly due to the contribution of forest improvement in Russia, where the increasing trend reached 32.79% and the decreasing trend was only 4.51%. In contrast, grassland exhibited both increasing and decreasing trends, which accounted for 14.31% and 18.09% of the total grassland, respectively. An increasing trend mainly appeared in Russia, while a decreasing trend predominantly occurred in Mongolia. For grassland regions in Mongolia, the decreasing trend (21.09%) became more dominant than the increasing trend (11.86%). In contrast, the increasing trend (21.64%) of grassland in Russia far outweighed the increasing trend (8.33%).

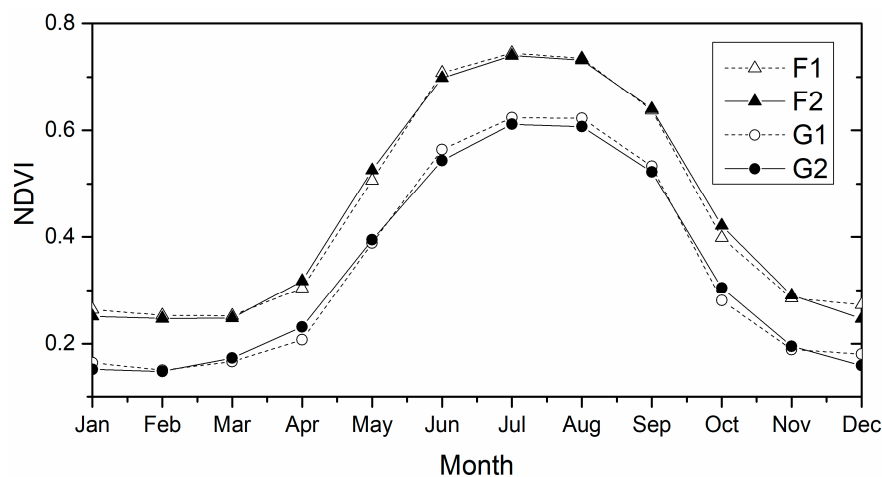


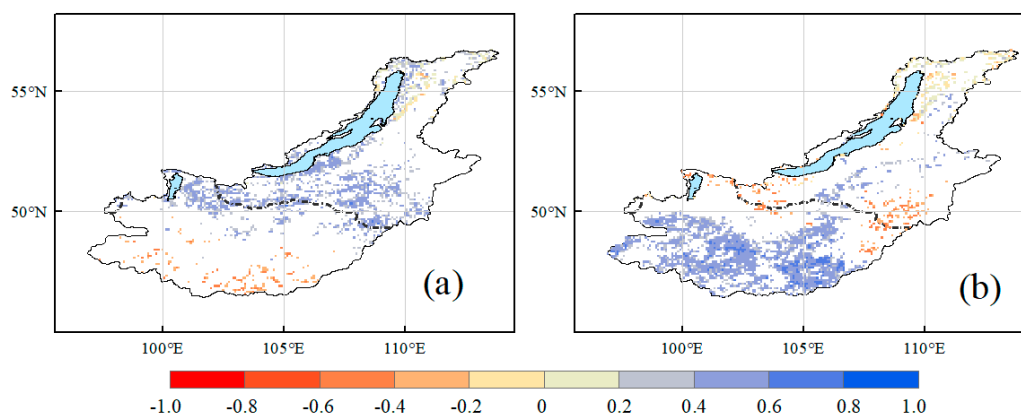
Figure 7. Annual NDVI time series for forest and grassland from 1982–1999 and 2000–2015. F1: forest during 1982–1999; F2: forest during 2000–2015; G1: grassland during 1982–1999; G2: grassland during 2000–2015.

Table 1. Statistical results of the NDVI change trend for different vegetation types in the growing season.

Trend	Forest			Grassland		
	All	Mongolia	Russia	All	Mongolia	Russia
Increasing (%)	30.19	18.13	32.79	14.31	11.86	21.64
Decreasing (%)	7.03	17.01	4.51	18.09	21.09	8.33
Insignificant (%)	62.78	64.86	62.70	67.60	67.05	70.03

3.3. Relationship between the NDVI and Climatic Factors

A partial correlation analysis was performed to evaluate responses of the NDVI to air temperature and precipitation. As shown in Figure 8, there were notable spatial differences in the partial correlation coefficients between the mean NDVI during the growing seasons and the annual temperature and precipitation. In general, the NDVI was negatively correlated with air temperature and positively correlated with precipitation in the southern part of the Selenga-Baikal Basin, which is within Mongolia. However, the NDVI was positively correlated with air temperature east of Lake Hovsgol, where the annual precipitation exceeds 400 mm (Figure 2). Additionally, the NDVI was negatively correlated with precipitation and positively correlated with temperature in the southeastern basin, which is near the national border between Mongolia and Russia.

**Figure 8.** Spatial distribution of the partial correlation coefficients ($p < 0.05$) (a) between the NDVI and temperature and (b) between the NDVI and precipitation.

Generally, the response of the NDVI to the changing climate is primarily associated with precipitation in the study region. As shown in Figure 8b and Table 2, 50.53% of the dry regions, where the average annual precipitation is less than 350 mm, exhibited a positive correlation ($p < 0.05$) between NDVI and precipitation. In addition, 4.65% of the dry regions showed a negative correlation ($p < 0.05$) between NDVI and temperature. In relatively wet regions, where the average annual precipitation is greater than 350 mm, the responses of NDVI to temperature and precipitation differ from those of the dry regions. According to the statistical analysis, 26.58% of the wet regions exhibited positive correlations ($p < 0.05$) between the NDVI and air temperature, and the area with a positive correlation between NDVI and precipitation (49.68%) was almost equal to the area with a negative correlation (50.32%), whereas only 8.59% and 5.72% of these regions exhibited significant ($p < 0.05$) positive and negative correlations, respectively.

Table 2. Partial correlation coefficients for the relationships between the NDVI and temperature (upper) and between the NDVI and precipitation (lower) in different water conditions.

Relationship	Correlation	The Dry Regions	The Wet Regions
NDVI and Temperature (%)	Positive	1.14	26.58
	Negative	4.65	0.89
	Insignificant	94.21	72.53
NDVI and Precipitation (%)	Positive	50.53	8.59
	Negative	0.40	5.72
	Insignificant	49.07	85.69

As shown in Table 3, the responses of forest and grassland to climate factors, i.e., air temperature and precipitation, varied markedly. A total of 25.81% of forest showed a significant positive correlation ($p < 0.05$) between the NDVI and temperature, as opposed to only 11.57% of forest. Compared with the forest areas, a greater area of grassland showed positive correlations between the NDVI and precipitation, which was observed in 33.68% of the grassland area ($p < 0.05$), whereas significant positive correlation ($p < 0.05$) between the NDVI and temperature were only observed in 6.95% of the grassland area.

Table 3. Partial correlation coefficients for the relationships between the NDVI and temperature (upper) and between the NDVI and precipitation (lower) in different vegetation types.

Relationship	Correlation	Forest (%)	Grassland (%)
NDVI and Temperature (%)	Positive	25.81	11.57
	Negative	0.81	2.79
	Insignificant	73.37	85.64
NDVI and Precipitation (%)	Positive	6.95	33.68
	Negative	5.32	2.73
	Insignificant	87.72	63.59

4. Discussion

4.1. Response of Vegetation to Climatic Variables between Dry and Wet Conditions

Globally, an overall greening trend (25% to 50%) has been detected in the earth terrestrial ecosystem, which could be mainly explained by CO₂ fertilization, nitrogen deposition, climate change, and land cover change [66]. However, the dominant factors that contribute to vegetation growth may be different at regional scales. In energy-limited regions, such as the Tibetan Plateau and other high-altitude areas, warming generally contributes the most effect to the greening [67–70], while as environment aridity increases, the water availability's impact on the vegetation dynamics is growing [71–74].

For the Selenga-Baikal Basin, which is an arid and semiarid region, vegetation responded differently to climatic variables under different hydrothermal conditions. In the dry regions where mean annual precipitation is less than 350 mm, vegetation growth is more sensitive to precipitation than temperature, and the vegetation decline is mostly associated with widespread drought stress [75–77]. Precipitation is the dominant factor influencing vegetation growth in such overall water-limited conditions [76,78,79], although in relatively wet regions where mean annual precipitation is greater than 350 mm, precipitation is usually a less-limiting factor. And even a negative relationship was observed between the NDVI and precipitation in regions with high precipitation, such as the Hovsgol area of the Selenga-Baikal Basin, which is consistent with previous studies, e.g., [19,77,80]. This anomalous relationship may be explained by the saturation effect of increasing precipitation on vegetation growth [80], wherein excessive precipitation inhibits growth. In addition, increasing precipitation leads to increased cloudiness and reduced incoming solar radiation, which is disadvantageous for

plant growth after moisture requirements are met [77]. In regions with low temperatures and relatively high precipitation, the spatiotemporal heterogeneity of the vegetation dynamics is mainly determined by variations in temperature [81]; therefore, the overall temperature-limited but wet conditions result in temperature having a more substantial impact on vegetation growth [82].

4.2. Response of Grassland and Forest to Temperature and Precipitation

The responses of vegetation growth to climatic variables present obvious regional differences. Precipitation was the dominant factor affecting the growth of coniferous forests and grasslands in Xinjiang, China [54]. However, grasslands exhibited relatively high positive correlations with precipitation and forest ecosystems, and were primarily limited by temperature in Northeast China [83]. In the Selenga-Baikal Basin, the result was consistent with that of previous studies in Northeast China. In general, grassland is characterized by a semiarid and continental climate, while forest is usually distributed in areas with relatively higher humidity; therefore, precipitation is likely to be the predominant vegetation growth-limiting factor in grassland [84], while temperature is the main factor affecting growth in forests [83], particularly in the cold temperate zone.

Precipitation is the dominant factor affecting the growth of grassland in the Selenga-Baikal Basin. A previous study in Mongolia found that summer precipitation is the primary factor constraining vegetation growth in grasslands [85], and decreased precipitation reduces the soil water content, which is not conducive to grassland growth. In addition, the thickening of the active layer and soil water infiltration due to climate warming and permafrost thawing may cause a drier upper soil layer and inhibit the growth of grassland vegetation, which has a shallow root system [86]. However, forests in cold areas of the Northern Hemisphere are overwhelmingly temperature dominated and insensitive to drought [87,88]. Increased temperature was the primary driver of forest greening [89], and tree growth has been widely regarded to be temperature sensitive [90–92]. Furthermore, permafrost is an important source of soil water for forests during summer [22,93], and higher summer temperatures lead to the melting of frozen soil, thereby supplying water to the forest. Therefore, warming may be beneficial to plant growth in forest regions [82].

4.3. Influence of Human Disturbances on Vegetation Dynamics

It should be noted that human disturbance is an important force driving ecosystem degradation combined with natural factors [94], and the intensification of human activities has induced dramatic changes in land use and seriously affected natural ecosystems [24]. The Selenga-Baikal Basin is currently facing land use changes due to urbanization, the expansion of agricultural activities, mining, rising livestock numbers, logging and wildfires in the context of global warming, and rapid economic expansion [95,96]. The population of Mongolia more than tripled since the second half of the 20th century, and it was accompanied by an increase in the proportion of the urban population from 35% to 68.5%, causing a considerable increase in the use of surface water resources [97]. As an important backbone of the regional economy, mining is a major water consumer that has caused increasing water abstraction and contaminant loads originating from mining sites [98]. As a result, the Selenga River, which originates in the mountainous regions of Mongolia and constitutes the largest tributary of Lake Baikal, has experienced a low-water period over the past two decades [99], and the vegetation along the Selenga River exhibited a decreasing trend in intermountain regions that coincided with the reduced water conditions [26].

Nomadism is still an important feature of rural lifestyles, and animal husbandry is the major source of income [96]. Livestock grazing, which contributes to ecosystem interference with the greatest intensity, and therefore has the most severe consequences, was the most serious disturbance in the grassland ecosystem [100], although vegetation degeneration in recent decades throughout Mongolia was severely promoted by frequent grazing [34,101–105]. Sources of forest degradation include fires, logging, and human disturbances to the living ground cover [106]. Frequent and increasing wildfires in recent years have had important impacts on forests, and between 1997 and 2000, forest fires occurred

over approximately 30,000 ha each year in Siberia and approximately 650,000 ha over Chita, based on a government report on the state of the environment [107]. Furthermore, the burned area increased by nearly 200 times in the forestry districts in the basin of the Khilok River, a tributary of the Selenga River, during the last two decades [108]. The accumulation of water-stressed periods during summer exacerbates the problem of water shortages in downstream areas and leads to a conversion of forest to grassland [95,109–111], and this transformation may be responsible for the decreasing NDVI values in summer in areas classified as forest.

5. Conclusions

This research revealed vegetation growth dynamics and their responses to climatic variables over the Selenga-Baikal Basin from 1982 to 2015. The majority of this basin experienced notably increased temperatures and decreased precipitation, although the vegetation dynamics exhibited high spatial heterogeneity mainly driven by climate change and human disturbances. In most water-limited areas, where multiyear mean annual precipitation was below 350 mm, vegetation growth was positively correlated with precipitation, whereas in the cold temperate zone, it was mainly sensitive to temperature. Temperature is a predominant growth-limiting factor for forest vegetation, whereas precipitation is the limiting factor for grassland. Additionally, vegetation of the Selenga-Baikal Basin is associated with human disturbances such as urbanization, mining, increased wildfires, illegal logging, and livestock overgrazing. Our results are helpful for understanding vegetation dynamics in the semiarid regions of mid-to-high latitudes and may play an important guiding role in vegetation and environmental protection against the background of global climate change.

Author Contributions: Conceptualization, C.-M.L.; methodology, Y.-C.Z. and T.-Y.W.; validation, N.M. and N.L.F.; data curation, G.W.; writing—original draft preparation, G.W.; writing—review and editing, P.W.; supervision, J.-J.Y. and C.-M.L.; funding acquisition, P.W. and J.-J.Y.

Funding: This research was funded by the Science and Technology Basic Resources Investigation Program of China (Nos. 2017FY101302, 2017FY101301), the Strategic Priority Research Program of the Chinese Academy of Sciences (No. XDA2003020101), the Key Project of the Chinese Academy of Sciences (No. ZDRW-ZS-2017-4), grants from the National Natural Science Foundation of China (No. 41671023, 41571029, 41801047, and 41271050) and the NSFC-RFBR Program 2018–2019 (Nos. 41811530084 and 18-55-53025 ГФЕН_a).

Acknowledgments: We would like to express our sincere gratitude to the United States Geological Survey and the team at NASA for providing data on the different vegetation types. We also thank the Climate Research Unit of the University of East Anglia for providing climate data. The authors gratefully acknowledge the anonymous Academic Editor and the anonymous reviewers for their valuable comments and suggestions that have led to substantial improvements over an earlier version of the manuscript.

Conflicts of Interest: The authors declare no conflicts of interest.

References

1. IPCC. *Climate Change 2013: The Physical Science Basis*; Cambridge University Press: Cambridge, UK; New York, NY, USA, 2013; Volume 43, pp. 866–871.
2. Jiang, L.; Jiapaer, G.; Bao, A.; Guo, H.; Ndayisaba, F. Vegetation dynamics and responses to climate change and human activities in Central Asia. *Sci. Total Environ.* **2017**, *599–600*, 967–980. [[CrossRef](#)] [[PubMed](#)]
3. Chou, C.; Chiang, J.C.H.; Lan, C.W.; Chung, C.H.; Liao, Y.C.; Lee, C.J. Increase in the range between wet and dry season precipitation. *Nat. Geosci.* **2013**, *6*, 263–267. [[CrossRef](#)]
4. Myneni, R.B.; Yang, W.; Nemani, R.R.; Huete, A.R.; Dickinson, R.E.; Knyazikhin, Y.; Didan, K.; Fu, R.; Juárez, R.I.N.; Saatchi, S.S. Large seasonal swings in leaf area of Amazon rainforests. *Proc. Natl. Acad. Sci. USA* **2007**, *104*, 4820–4823. [[CrossRef](#)] [[PubMed](#)]
5. Bachelet, D.; Neilson, R.P.; Lenihan, J.M.; Drapek, R.J. Climate change effects on vegetation distribution and carbon budget in the United States. *Ecosystems* **2001**, *4*, 164–185. [[CrossRef](#)]
6. Cao, M.; Woodward, F.I. Dynamic responses of terrestrial ecosystem carbon cycling to global climate change. *Nature* **1998**, *393*, 249–252. [[CrossRef](#)]

7. Cramer, W.; Bondeau, A.; Woodward, F.I.; Prentice, I.C.; Betts, R.A.; Brovkin, V.; Cox, P.M.; Fisher, V.; Foley, J.A.; Friend, A.D. Global response of terrestrial ecosystem structure and function to CO₂ and climate change: Results from six dynamic global vegetation models. *Glob. Chang. Biol.* **2001**, *7*, 357–373. [[CrossRef](#)]
8. Schneider, R.R.S.R.; Hamann, A.H.; Farr, D.F.; Wang, X.W.; Boutin, S.B. Potential effects of climate change on ecosystem distribution in Alberta. *Can. J. For. Res.* **2009**, *39*, 1001–1010. [[CrossRef](#)]
9. Theurillat, J.P.; Guisan, A. Potential impact of climate change on vegetation in the European Alps: A review. *Clim. Chang.* **2001**, *50*, 77–109. [[CrossRef](#)]
10. Piao, S.; Fang, J.; Ji, W.; Guo, Q.; Ke, J.; Tao, S. Variation in a satellite-based vegetation index in relation to climate in China. *J. Veg. Sci.* **2004**, *15*, 219–226. [[CrossRef](#)]
11. Chase, T.N.; Pielke, R.A., Sr.; Knaff, J.A.; Kittel, T.G.F.; Eastman, J.L. A comparison of regional trends in 1979–1997 depth-averaged tropospheric temperatures. *Int. J. Climatol.* **2000**, *20*, 503–518. [[CrossRef](#)]
12. Zhang, H.-X.; Zhang, M.-L.; Sanderson, S.C. Retreating or standing: Responses of forest species and steppe species to climate change in arid eastern Central Asia. *PLoS ONE* **2013**, *8*, e61954. [[CrossRef](#)]
13. Yu, F.; Price, K.P.; Ellis, J.; Shi, P. Response of seasonal vegetation development to climatic variations in eastern Central Asia. *Remote Sens. Environ.* **2003**, *87*, 42–54. [[CrossRef](#)]
14. Liu, S.L.; Wang, T.; Guo, J.; Qu, J.J.; An, P.J. Vegetation change based on spot-vgt data from 1998 to 2007, northern China. *Environ. Earth Sci.* **2010**, *60*, 1467–1468. [[CrossRef](#)]
15. Peng, J.; Liu, Z.; Liu, Y.; Wu, J.; Han, Y. Trend analysis of vegetation dynamics in Qinghai–Tibet Plateau using Hurst Exponent. *Ecol. Indic.* **2012**, *14*, 28–39. [[CrossRef](#)]
16. Wu, D.; Zhao, X.; Liang, S.; Zhou, T.; Huang, K.; Tang, B.; Zhao, W. Time-lag effects of global vegetation responses to climate change. *Glob. Chang. Biol.* **2015**, *21*, 3520–3531. [[CrossRef](#)] [[PubMed](#)]
17. Jeong, S.J.; Ho, C.H.; Gim, H.J.; Brown, M.E. Phenology shifts at start vs. End of growing season in temperate vegetation over the Northern Hemisphere for the period 1982–2008. *Glob. Chang. Biol.* **2011**, *17*, 2385–2399. [[CrossRef](#)]
18. Craine, J.M.; Nippert, J.B.; Elmore, A.J.; Skibbe, A.M.; Hutchinson, S.L.; Brunsell, N.A. Timing of climate variability and grassland productivity. *Proc. Natl. Acad. Sci. USA* **2012**, *109*, 3401–3405. [[CrossRef](#)]
19. Nemani, R.R.; Keeling, C.D.; Hashimoto, H.; Jolly, W.M.; Piper, S.C.; Tucker, C.J.; Myneni, R.B.; Running, S.W. Climate-driven increases in global terrestrial net primary production from 1982 to 1999. *Science* **2003**, *300*, 1560–1563. [[CrossRef](#)]
20. Beer, C.; Reichstein, M.; Tomelleri, E.; Ciais, P.; Jung, M.; Carvalhais, N.; Rödenbeck, C.; Arain, M.A.; Baldocchi, D.; Bonan, G.B. Terrestrial gross carbon dioxide uptake: Global distribution and covariation with climate. *Science* **2010**, *329*, 834–838. [[CrossRef](#)]
21. Wang, X.; Piao, S.; Ciais, P.; Li, J.; Friedlingstein, P.; Koven, C.; Chen, A. Spring temperature change and its implication in the change of vegetation growth in North America from 1982 to 2006. *Proc. Natl. Acad. Sci. USA* **2011**, *108*, 1240–1245. [[CrossRef](#)]
22. Törnqvist, R.; Jarsjö, J.; Pietroń, J.; Bring, A.; Rogberg, P.; Asokan, S.M.; Destouni, G. Evolution of the hydro-climate system in the Lake Baikal Basin. *J. Hydrol.* **2014**, *519*, 1953–1962. [[CrossRef](#)]
23. Frolova, N.L.; Belyakova, P.A.; Grigor'Ev, V.Y.; Sazonov, A.A.; Zotov, L.V. Many-year variations of river runoff in the Selenga Basin. *Water Resour.* **2017**, *44*, 359–371. [[CrossRef](#)]
24. Hirano, A.; Batbileg, B. Identifying trends in the distribution of vegetation in Mongolia in the decade after its transition to a market economy. *Jpn. Agric. Res. Q. Jarq* **2013**, *47*, 203–208. [[CrossRef](#)]
25. Maksimova, I.I. Using the status of a world heritage site for the preservation of Lake Baikal. *Geogr. Nat. Resour.* **2013**, *34*, 124–128. [[CrossRef](#)]
26. Dorjsuren, B.; Yan, D.; Wang, H.; Chonokhuu, S.; Enkhbold, A.; Yiran, X.; Girma, A.; Gedefaw, M.; Abiyu, A. Observed trends of climate and river discharge in Mongolia's Selenga Sub-Basin of the Lake Baikal Basin. *Water* **2018**, *10*, 1436. [[CrossRef](#)]
27. Dobrovol'skii, S.G. Year-to-year and many-year river runoff variations in Baikal Drainage Basin. *Water Resour.* **2017**, *44*, 347–358. [[CrossRef](#)]
28. Moore, M.V.; Hampton, S.E.; Izmet'eva, L.R.; Silow, E.A.; Peshkova, E.V.; Pavlov, B.K. Climate change and the world's "sacred sea"—Lake Baikal, Siberia. *Bioscience* **2009**, *59*, 405–417. [[CrossRef](#)]
29. Karthe, D.; Chalov, S.; Kasimov, N.; Kappas, M. *Water and Environment in the Selenga-Baikal Basin: International Research Cooperation for an Ecoregion of Global Relevance*; ibidem-Verlag: Stuttgart, Germany, 2015; p. 57.

30. Karthe, D.; Kasimov, N.S.; Chalov, S.R.; Shinkareva, G.L.; Malsy, M.; Menzel, L.; Theuring, P.; Hartwig, M.; Schweitzer, C.; Hofmann, J.; et al. Integrating multi-scale data for the assessment of water availability and quality in the Kharaa-Orkhon-Selenga river system. *Geogr. Environ. Sustain.* **2014**, *7*, 65–86. [[CrossRef](#)]
31. Kozhova, O.M.; Izmet'eva, L.R.; Levinton, J. *Lake Baikal: Evolution and Biodiversity*; Leiden: Backhuys, The Netherlands, 1998; p. 447.
32. Kopp, B.J.; Minderlein, S.; Menzel, L. Soil moisture dynamics in a mountainous headwater area in the discontinuous permafrost zone of Northern Mongolia. *Arct. Antarct. Alp. Res.* **2014**, *46*, 459–470. [[CrossRef](#)]
33. Dugarsuren, N.; Lin, C. Temporal variations in phenological events of forests, grasslands and desert steppe ecosystems in Mongolia: A remote sensing approach. *Ann. For. Res.* **2016**, *59*, 175–190.
34. Hilker, T.; Natsagdorj, E.; Waring, R.H.; Lyapustin, A.; Wang, Y. Satellite observed widespread decline in Mongolian grasslands largely due to overgrazing. *Glob. Chang. Biol.* **2014**, *20*, 418–428. [[CrossRef](#)]
35. Harris, I.; Jones, P.D.; Osborn, T.J.; Lister, D.H. Updated high-resolution grids of monthly climatic observations—The CRU TS3.10 dataset. *Int. J. Climatol.* **2014**, *34*, 623–642. [[CrossRef](#)]
36. New, M.; Hulme, M.; Jones, P. Representing twentieth-century space-time climate variability. Part II: Development of 1901–96 monthly grids of terrestrial surface climate. *J. Clim.* **2000**, *12*, 829–856. [[CrossRef](#)]
37. Mitchell, T.D.; Jones, P.D. An improved method of constructing a database of monthly climate observations and associated high-resolution grids. *Int. J. Climatol.* **2005**, *25*, 693–712. [[CrossRef](#)]
38. Moberg, A.; Jones, P.D.; Lister, D.; Walther, A.; Brunet, M.; Jacobeit, J.; Alexander, L.V.; Della-Marta, P.M.; Luterbacher, J.; Yiou, P. Indices for daily temperature and precipitation extremes in Europe analyzed for the period 1901–2000. *J. Geophys. Res. Atmos.* **2006**, *111*, 5295–5305. [[CrossRef](#)]
39. Xu, X.; Liu, W.; Scanlon, B.R.; Zhang, L.; Pan, M. Local and global factors controlling water-energy balances within the budyko framework. *Geophys. Res. Lett.* **2013**, *40*, 6123–6129. [[CrossRef](#)]
40. Chen, J.; Chen, J.; Liao, A.; Cao, X.; Chen, L.; Chen, X.; He, C.; Han, G.; Peng, S.; Lu, M. Global land cover mapping at 30 m resolution: A pok-based operational approach. *ISPRS J. Photogramm. Remote Sens.* **2015**, *103*, 7–27. [[CrossRef](#)]
41. Ye, X.; Zhao, J.; Huang, L.; Zhang, D.; Hong, Q. *A Comparison of Four Global Land Cover Maps on a Provincial Scale Based on China's 30 m GlobeLand30*; Springer: Singapore, 2017; pp. 447–455.
42. Tan, S.; Xu, Z.; Peng, T. A comparative study on effects of spatial aggregation for GlobeLand30. In Proceedings of the 2015 23rd International Conference on Geoinformatics, Wuhan, China, 19–21 June 2015; pp. 1–4.
43. Chen, J.; Liao, A.; Chen, J.; Peng, S.; Chen, L.; Zhang, H. 30-meter global land cover data product- Globe Land30. *Geomat. World* **2017**, *24*, 1–8.
44. Wu, X.; Liu, H.; Li, X.; Piao, S.; Ciais, P.; Guo, W.; Yin, Y.; Poulter, B.; Peng, C.; Viovy, N. Higher temperature variability reduces temperature sensitivity of vegetation growth in Northern Hemisphere. *Geophys. Res. Lett.* **2017**, *44*. [[CrossRef](#)]
45. Piao, S.; Nan, H.; Huntingford, C.; Ciais, P.; Friedlingstein, P.; Sitch, S.; Peng, S.; Ahlström, A.; Canadell, J.G.; Cong, N.; et al. Evidence for a weakening relationship between interannual temperature variability and northern vegetation activity. *Nat. Commun.* **2014**, *5*, 5018. [[CrossRef](#)]
46. Jong, R.D.; Verbesselt, J.; Zeileis, A.; Schaepman, M.E. Shifts in global vegetation activity trends. *Remote Sens.* **2013**, *5*, 1117–1133. [[CrossRef](#)]
47. Mao, J.; Shi, X.; Thornton, P.E.; Hoffman, F.M.; Zhu, Z.; Myneni, R.B. Global latitudinal-asymmetric vegetation growth trends and their driving mechanisms: 1982–2009. *Remote Sens.* **2013**, *5*, 1484–1497. [[CrossRef](#)]
48. Wu, D.; Wu, H.; Zhao, X.; Zhou, T.; Tang, B.; Zhao, W.; Jia, K. Evaluation of spatio-temporal variations of global fractional vegetation cover based on GIMMS NDVI data from 1982 to 2011. *Remote Sens.* **2014**, *6*, 4217–4239. [[CrossRef](#)]
49. Buermann, W.; Parida, B.; Jung, M.; Macdonald, G.M.; Tucker, C.J.; Reichstein, M. Recent shift in Eurasian boreal forest greening response may be associated with warmer and drier summers. *Geophys. Res. Lett.* **2014**, *41*, 1995–2002. [[CrossRef](#)]
50. Holben, B. Characteristics of maximum-value composite images from temporal AVHRR data. *Int. J. Remote Sens.* **1986**, *7*, 1417–1434. [[CrossRef](#)]
51. Beck, P.S.A.; Atzberger, C.; Høgda, K.A.; Johansen, B.; Skidmore, A.K. Improved monitoring of vegetation dynamics at very high latitudes: A new method using MODIS NDVI. *Remote Sens. Environ.* **2006**, *100*, 321–334. [[CrossRef](#)]

52. Lavrentyeva, I.N.; Merkusheva, M.G.; Ubugunov, L.L. Evaluation of organic carbon stocks and CO₂ fluxes in grasslands of Western Transbaikalia. *Eurasian Soil Sci.* **2017**, *50*, 396–411. [[CrossRef](#)]
53. Cao, R.; Jiang, W.; Yuan, L.; Wang, W.; Lv, Z.; Chen, Z. Inter-annual variations in vegetation and their response to climatic factors in the upper catchments of the Yellow River from 2000 to 2010. *J. Geogr. Sci.* **2014**, *24*, 963–979. [[CrossRef](#)]
54. Guli-Jiapaer; Liang, S.; Yi, Q.; Liu, J. Vegetation dynamics and responses to recent climate change in Xinjiang using leaf area index as an indicator. *Ecol. Indic.* **2015**, *58*, 64–76.
55. Fensholt, R.; Langanke, T.; Rasmussen, K.; Reenberg, A.; Prince, S.D.; Tucker, C.; Scholes, R.J.; Le, Q.B.; Bondeau, A.; Eastman, R. Greenness in semi-arid areas across the globe 1981–2007—An earth observing satellite based analysis of trends and drivers. *Remote Sens. Environ.* **2012**, *121*, 144–158. [[CrossRef](#)]
56. Lunetta, R.S.; Knight, J.F.; Ediriwickrema, J. Land-cover characterization and change detection using multitemporal MODIS NDVI data. *Remote Sens. Environ.* **2006**, *105*, 142–154. [[CrossRef](#)]
57. Milich, L.; Weiss, E. GAC NDVI interannual coefficient of variation (CoV) images: Ground truth sampling of the Sahel along north-south transects. *Int. J. Remote Sens.* **2000**, *21*, 235–260. [[CrossRef](#)]
58. Kendall, M.G. *Rank Correlation Methods*, 2nd ed.; Charles Griffin: London, UK, 1955; pp. 1–196.
59. Mann, H.B. Nonparametric test against trend. *Econometrica* **1945**, *13*, 245–259. [[CrossRef](#)]
60. Fuller, D.O.; Wang, Y. Recent trends in satellite vegetation index observations indicate decreasing vegetation biomass in the Southeastern Saline Everglades wetlands. *Wetlands* **2014**, *34*, 67–77. [[CrossRef](#)]
61. Fensholt, R.; Proud, S.R. Evaluation of Earth Observation based global long term vegetation trends—Comparing GIMMS and MODIS global NDVI time series. *Remote Sens. Environ.* **2012**, *119*, 131–147. [[CrossRef](#)]
62. Hazewinkel, M. Encyclopaedia of mathematics. *Ref. Rev.* **1987**, *17*, 49–50.
63. Khazheeva, Z.I.; Plyusnin, A.M. Variations in climatic and hydrological parameters in the Selenga River Basin in the Russian Federation. *Russ. Meteorol. Hydrol.* **2016**, *41*, 640–647. [[CrossRef](#)]
64. Dashkhuu, D.; Kim, J.P.; Chun, J.A.; Lee, W.-S. Long-term trends in daily temperature extremes over Mongolia. *Weather Clim. Extrem.* **2015**, *8*, 26–33. [[CrossRef](#)]
65. Obyazov, V.A.; Smakhtin, V.K. Climate change effects on winter river runoff in Transbaikalia. *Russ. Meteorol. Hydrol.* **2013**, *38*, 503–508. [[CrossRef](#)]
66. Zhu, Z.C.; Piao, S.L.; Myneni, R.B.; Huang, M.T.; Zeng, Z.Z.; Canadell, J.G.; Ciais, P.; Sitch, S.; Friedlingstein, P.; Arneeth, A.; et al. Greening of the earth and its drivers. *Nat. Clim. Chang.* **2016**, *6*, 791–795. [[CrossRef](#)]
67. Li, Y.; Zeng, Z.; Huang, L.; Lian, X.; Piao, S. Comment on “satellites reveal contrasting responses of regional climate to the widespread greening of earth”. *Science* **2018**, *360*. [[CrossRef](#)] [[PubMed](#)]
68. Zhang, G.; Zhang, Y.; Dong, J.; Xiao, X. Green-up dates in the Tibetan Plateau have continuously advanced from 1982 to 2011. *Proc. Natl. Acad. Sci. USA* **2013**, *110*, 4309–4314. [[CrossRef](#)]
69. Keenan, T.F.; Riley, W.J. Greening of the land surface in the world’s cold regions consistent with recent warming. *Nat. Clim. Chang.* **2018**, *8*, 825–828. [[CrossRef](#)]
70. Peng, S.; Piao, S.; Ciais, P.; Myneni, R.B.; Chen, A.; Chevallier, F.; Dolman, A.J.; Janssens, I.A.; Penuelas, J.; Zhang, G.; et al. Asymmetric effects of daytime and night-time warming on Northern Hemisphere vegetation. *Nature* **2013**, *501*, 88–92. [[CrossRef](#)]
71. Sohoulane Djebou, D.C.; Singh, V.P.; Frauenfeld, O.W. Vegetation response to precipitation across the aridity gradient of the Southwestern United States. *J. Arid Environ.* **2015**, *115*, 35–43. [[CrossRef](#)]
72. Schlaepfer, D.R.; Bradford, J.B.; Lauenroth, W.K.; Munson, S.M.; Tietjen, B.; Hall, S.A.; Wilson, S.D.; Duniway, M.C.; Jia, G.; Pyke, D.A.; et al. Climate change reduces extent of temperate drylands and intensifies drought in deep soils. *Nat. Commun.* **2017**, *8*, 14196. [[CrossRef](#)]
73. Yu, Y.; Notaro, M.; Wang, F.; Mao, J.; Shi, X.; Wei, Y. Observed positive vegetation-rainfall feedbacks in the Sahel dominated by a moisture recycling mechanism. *Nat. Commun.* **2017**, *8*, 1873. [[CrossRef](#)] [[PubMed](#)]
74. Shen, M.; Piao, S.; Cong, N.; Zhang, G.; Janssens, I.A. Precipitation impacts on vegetation spring phenology on the Tibetan Plateau. *Glob. Chang. Biol.* **2015**, *21*, 3647–3656. [[CrossRef](#)] [[PubMed](#)]
75. Bao, G.; Qin, Z.; Bao, Y.; Zhou, Y.; Li, W.; Sanjiv, A. NDVI-based long-term vegetation dynamics and its response to climatic change in the Mongolian Plateau. *Remote Sens.* **2014**, *6*, 8337–8358. [[CrossRef](#)]
76. Wei, H.; Zhao, X.; Liang, S.; Zhou, T.; Wu, D.; Tang, B. Effects of warming hiatuses on vegetation growth in the Northern Hemisphere. *Remote Sens.* **2018**, *10*, 683. [[CrossRef](#)]

77. Song, Y.; Ma, M. A statistical analysis of the relationship between climatic factors and the Normalized Difference Vegetation Index in China. *Int. J. Remote Sens.* **2011**, *32*, 3947–3965. [[CrossRef](#)]
78. Ukkola, A.M.; Prentice, I.C.; Keenan, T.F.; van Dijk, A.I.J.M.; Viney, N.R.; Myneni, R.B.; Bi, J. Reduced streamflow in water-stressed climates consistent with CO₂ effects on vegetation. *Nat. Clim. Chang.* **2015**, *6*, 75. [[CrossRef](#)]
79. Ichii, K.; Kawabata, A.; Yamaguchi, Y. Global correlation analysis for NDVI and climatic variables and NDVI trends: 1982–1990. *Int. J. Remote Sens.* **2002**, *23*, 3873–3878. [[CrossRef](#)]
80. Nicholson, S.E.; Davenport, M.L.; Malo, A.R. A comparison of the vegetation response to rainfall in the Sahel and East Africa, using normalized difference vegetation index from NOAA AVHRR. *Clim. Chang.* **1990**, *17*, 209–241. [[CrossRef](#)]
81. Chu, T.; Guo, X. Characterizing vegetation response to climatic variations in Hovsgol, Mongolia using remotely sensed time series data. *Earth Sci. Res.* **2012**, *1*, 279–290. [[CrossRef](#)]
82. Berner, L.T.; Beck, P.S.; Bunn, A.G.; Goetz, S.J. Plant response to climate change along the forest-tundra ecotone in Northeastern Siberia. *Glob. Chang. Biol.* **2013**, *19*, 3449–3462. [[CrossRef](#)] [[PubMed](#)]
83. Jing, P.; Dong, W.; Yuan, W.; Yong, Z. Responses of grassland and forest to temperature and precipitation changes in Northeast China. *Adv. Atmos. Sci.* **2012**, *29*, 1063–1077.
84. Fang, J.; Piao, S.; Zhou, L.; He, J.; Wei, F.; Myneni, R.B.; Tucker, C.J.; Tan, K. Precipitation patterns alter growth of temperate vegetation. *Geophys. Res. Lett.* **2005**, *32*, 365–370. [[CrossRef](#)]
85. Gantsetseg, B.; Ishizuka, M.; Kurosaki, Y.; Mikami, M. Topographical and hydrological effects on meso-scale vegetation in desert steppe, Mongolia. *J. Arid Land* **2017**, *9*, 132–142. [[CrossRef](#)]
86. Xue, X.; Guo, J.; Han, B.; Sun, Q.; Liu, L. The effect of climate warming and permafrost thaw on desertification in the Qinghai–Tibetan Plateau. *Geomorphology* **2009**, *108*, 182–190. [[CrossRef](#)]
87. Huang, L.; He, B.; Chen, A.; Wang, H.; Liu, J.; Lü, A.; Chen, Z. Drought dominates the interannual variability in global terrestrial net primary production by controlling semi-arid ecosystems. *Sci. Rep.* **2016**, *6*, 24639. [[CrossRef](#)] [[PubMed](#)]
88. Vicente-Serrano, S.M.; Gouveia, C.; Camarero, J.J.; Beguería, S.; Trigo, R.; López-Moreno, J.I.; Azorín-Molina, C.; Pasho, E.; Lorenzo-Lacruz, J.; Revuelto, J.; et al. Response of vegetation to drought time-scales across global land biomes. *Proc. Natl. Acad. Sci. USA* **2013**, *110*, 52–57. [[CrossRef](#)] [[PubMed](#)]
89. Qi, Z.; Liu, H.; Wu, X.; Hao, Q. Climate-driven speedup of alpine treeline forest growth in the Tianshan Mountains, Northwestern China. *Glob. Chang. Biol.* **2015**, *21*, 816–826. [[CrossRef](#)] [[PubMed](#)]
90. Salzer, M.W.; Hughes, M.K.; Bunn, A.G.; Kipfmüller, K.F. Recent unprecedented tree-ring growth in bristlecone pine at the highest elevations and possible causes. *Proc. Natl. Acad. Sci. USA* **2009**, *106*, 20348–20353. [[CrossRef](#)] [[PubMed](#)]
91. Zhang, X.; Tarpley, D.; Sullivan, J.T. Diverse responses of vegetation phenology to a warming climate. *Geophys. Res. Lett.* **2007**, *34*, L19405. [[CrossRef](#)]
92. Briffa, K.R.; Shishov, V.; Melvin, T.; Vaganov, E.A.; Grudd, H.; Hantemirov, R.M.; Eronen, M.; Naurzbaev, M.M. Trends in recent temperature and radial tree growth spanning 2000 years across Northwest Eurasia. *Philos. Trans. R. Soc. Lond. B Biol. Sci.* **2008**, *363*, 2271–2284. [[CrossRef](#)] [[PubMed](#)]
93. Grippa, M.; Kergoat, L.; Toan, T.L.; Mognard, N.M.; Delbart, N.; L’Hermitte, J.; Vicente-Serrano, S.M. The impact of snow depth and snowmelt on the vegetation variability over Central Siberia. *Geophys. Res. Lett.* **2005**, *32*, 365–370. [[CrossRef](#)]
94. Vitousek, P.M.; Mooney, H.A.; Lubchenco, J.; Melillo, J.M. Human domination of earth’s ecosystems. *Science* **1997**, *277*, 494–499. [[CrossRef](#)]
95. Minderlein, S.; Menzel, L. Evapotranspiration and energy balance dynamics of a semi-arid mountainous steppe and shrubland site in Northern Mongolia. *Environ. Earth Sci.* **2015**, *73*, 593–609. [[CrossRef](#)]
96. Karthe, D.; Heldt, S.; Houdret, A.; Borchardt, D. Iwrm in a country under rapid transition: Lessons learnt from the Kharaa River Basin, Mongolia. *Environ. Earth Sci.* **2015**, *73*, 681–695. [[CrossRef](#)]
97. Batsukh, N.; Dorjsuren, D.; Batsaikan, G. *The Water Resources, Use and Conservation in Mongolia (First Nation Report)*; National Water Committee of Mongolia, Mongolian Ministry of Nature and Environment: Ulaanbaatar, Mongolia, 2008; p. 40.
98. Karthe, D.; Chalov, S.; Moreido, V.; Pashkina, M.; Romanchenko, A.; Batbayar, G.; Kalugin, A.; Westphal, K.; Malsy, M.; Flörke, M. Assessment of runoff, water and sediment quality in the Selenga River Basin aided by a web-based geoservice. *Water Resour.* **2017**, *44*, 399–416. [[CrossRef](#)]

99. Moreido, V.M.; Kalugin, A.S. Assessing possible changes in selenga r. Water regime in the XXI century based on a runoff formation model. *Water Resour.* **2017**, *44*, 390–398. [[CrossRef](#)]
100. Liu, Y.Y.; Evans, J.P.; McCabe, M.F.; Jeu, R.A.M.D.; Dijk, A.I.J.M.V.; Dolman, A.J.; Saizen, I. Changing climate and overgrazing are decimating Mongolian steppes. *PLoS ONE* **2013**, *8*, e57599. [[CrossRef](#)] [[PubMed](#)]
101. Karthe, D. Environmental changes in Central and East Asian drylands and their effects on major river-lake systems. *Quat. Int.* **2017**, 1–10. [[CrossRef](#)]
102. Fernández-Giménez, M.E.; Allington, G.R.H.; Angerer, J.; Reid, R.S.; Jamsranjav, C.; Ulambayar, T.; Hondula, K.; Baival, B.; Batjav, B.; Altanzul, T. Using an integrated social-ecological analysis to detect effects of household herding practices on indicators of rangeland resilience in Mongolia. *Environ. Res. Lett.* **2018**, *13*, 075010. [[CrossRef](#)]
103. Fernández-Giménez, M.E.; Venable, N.H.; Angerer, J.; Fassnacht, S.R.; Reid, R.S.; Khishigbayar, J. Exploring linked ecological and cultural tipping points in Mongolia. *Anthropocene* **2017**, *17*, 46–69. [[CrossRef](#)]
104. John, R.; Chen, J.; Giannico, V.; Park, H.; Xiao, J.; Shirkey, G.; Ouyang, Z.; Shao, C.; Laforteza, R.; Qi, J. Grassland canopy cover and aboveground biomass in Mongolia and Inner Mongolia: Spatiotemporal estimates and controlling factors. *Remote Sens. Environ.* **2018**, *213*, 34–48. [[CrossRef](#)]
105. John, R.; Chen, J.; Kim, Y.; Ou-Yang, Z.T.; Xiao, J.; Park, H.; Shao, C.; Zhang, Y.; Amarjargal, A.; Batkhshig, O. Differentiating anthropogenic modification and precipitation-driven change on vegetation productivity on the Mongolian Plateau. *Landsc. Ecol.* **2016**, *31*, 547–566. [[CrossRef](#)]
106. Vedrova, E.F.; Mukhortova, L.V.; Ivanov, V.V.; Krivobokov, L.V.; Boloneva, M.V. Post-logging organic matter recovery in forest ecosystems of eastern Baikal Region. *Biol. Bull.* **2010**, *37*, 69–79. [[CrossRef](#)]
107. Shcherbov, B.L.; Strakhovenko, V.D.; Sukhorukov, F.V. The ecogeochemical role of forest fires in the Baikal region. *Geogr. Nat. Resour.* **2008**, *29*, 150–155. [[CrossRef](#)]
108. Bagova, V.Z.; Faleichik, L.M. Forest fires in the Khilok River Basin. *Geogr. Nat. Resour.* **2006**, 54–59.
109. Hofmann, J.; Watson, V.; Scharaw, B. Groundwater quality under stress: Contaminants in the Kharaa River Basin (Mongolia). *Environ. Earth Sci.* **2015**, *73*, 629–648. [[CrossRef](#)]
110. Dulamsuren, C.; Hauck, M.; Leuschner, C. Recent drought stress leads to growth reductions in *larix sibirica* in the Western Khentey, Mongolia. *Glob. Chang. Biol.* **2010**, *16*, 3024–3035. [[CrossRef](#)]
111. Dulamsuren, C.; Hauck, M.; Mühlenberg, M. Insect and small mammal herbivores limit tree establishment in Northern Mongolian steppe. *Plant Ecol.* **2008**, *195*, 143–156. [[CrossRef](#)]



© 2019 by the authors. Licensee MDPI, Basel, Switzerland. This article is an open access article distributed under the terms and conditions of the Creative Commons Attribution (CC BY) license (<http://creativecommons.org/licenses/by/4.0/>).